Copper is an endogenous modulator of neural circuit spontaneous activity

Sheel C. Dodani[a,1], Alana Firl[b,1], Jefferson Chan[a,1], Christine I. Nam[a,c], Allegra T. Aron[a], Carl S. Onak[a], Karla M. Ramos-Torres[a], Jaeho Paek[a], Corey M. Webster[d], Marla B. Feller[d,e], and Christopher J. Chang[a,c,d,e,2]

Departments of [a]Chemistry and [d]Molecular and Cell Biology, [b]Vision Sciences Graduate Program, Department of Optometry, [e]Helen Wills Neuroscience Institute, and [c]Howard Hughes Medical Institute, University of California, Berkeley, CA 94720

Edited by Harry B. Gray, California Institute of Technology, Pasadena, CA, and approved October 7, 2014 (received for review May 28, 2014)

For reasons that remain insufficiently understood, the brain requires among the highest levels of metals in the body for normal function. The traditional paradigm for this organ and others is that fluxes of alkali and alkaline earth metals are required for signaling, but transition metals are maintained in static, tightly bound reservoirs for metabolism and protection against oxidative stress. Here we show that copper is an endogenous modulator of spontaneous activity, a property of functional neural circuitry. Using Copper Fluor-3 (CF3), a new fluorescent Cu^+ sensor for one- and two-photon imaging, we show that neurons and neural tissue maintain basal stores of loosely bound copper that can be attenuated by chelation, which define a labile copper pool. Targeted disruption of these labile copper stores by acute chelation or genetic knockdown of the CTR1 (copper transporter 1) copper channel alters the spatiotemporal properties of spontaneous activity in developing hippocampal and retinal circuits. The data identify an essential role for copper neuronal function and suggest broader contributions of this transition metal to cell signaling.

copper signaling | fluorescent sensor | molecular imaging | neural activity

The foundation of cellular signal transduction relies on intricate chemical messenger systems that operate through the dynamic spatial and temporal regulation of elements, ions, and molecules. Nowhere is this concept better illustrated than in the brain, which extensively regulates fluxes of alkali and alkaline earth metals such as sodium, potassium, and calcium for a diverse array of signaling processes. Interestingly, the brain also accumulates among the highest levels of transition metals in the body (1–3), including redox-active copper. This high-redox metal load, in combination with the brain's disproportionately active oxygen metabolism (4), makes this organ particularly susceptible to oxidative stress (4–6). As such, copper has been historically regarded as a tightly sequestered cofactor that must be buried within protein active sites to protect against reactive oxygen species generation and subsequent free radical damage chemistry. Indeed, elegant work continues to identify molecular players that maintain copper homeostasis in the brain (7, 8) and related organs (9–11), and loss of this strict regulation is implicated in neurotoxic stress (12–14) and a variety of neurodegenerative and neurodevelopmental disorders including Menkes (15, 16) and Wilson's (17) diseases, familial amyotrophic lateral sclerosis (18, 19), Alzheimer's (6, 14, 20–22) and Huntington's (23, 24) diseases, and prion-mediated encephalopathies (14, 25, 26).

Despite this long-held paradigm, emerging data also link pools of labile copper (defined as dynamic and loosely bound stores that undergo facile ligand exchange relative to static, tightly bound pools buried within protein active sites) to neurophysiology. Included are observations of ^{64}Cu efflux from stimulated neurons (12, 27), reversible trafficking of ATP7A from the perinuclear trans-Golgi to neuronal processes by NMDA receptor activation (12), effects of copper chelation on olfactory response to thiol odorants (28), and direct X-ray fluorescence imaging of copper translocation in neurons from somatic cell bodies to peripheral processes upon depolarization (29). Against this backdrop, we have initiated a program aimed at exploring the potential contributions of loosely bound forms of redox-active metals like copper in cell signaling. In this report, we identify a role for copper in the brain as a modulator of spontaneous activity, a fundamental property of developing neural circuits. The design and synthesis of Copper Fluor-3 (CF3), a fluorescent copper sensor based on a hydrophilic and tunable rhodol scaffold, along with Control Copper Fluor-3 (Ctrl-CF3), a matched control dye based on an identical fluorophore but lacking responsiveness to copper, enabled the visualization of loosely bound Cu^+ in dissociated neurons and neural tissue by one- and two-photon microscopy. Disruption of Cu^+ stores by acute application of a copper chelator or genetic knockdown of the copper ion channel CTR1 altered the spatiotemporal properties of spontaneous activity. In dissociated hippocampal cultures, these manipulations increased the correlation of spontaneous calcium transients, whereas in retina, both cell participation and frequency of correlated calcium transients increased.

Results and Discussion

Design, Synthesis, and Evaluation of Rhodol-Based Fluorescent Copper Sensors Copper Rhodol-3 and CF3. We previously used X-ray fluorescence microscopy for direct total copper detection, inspired by initial pilot data using the BODIPY (boron dipyrromethene)-based fluorescent probe Coppersensor-3 (CS3) for labile Cu^+ imaging, to identify that dissociated cultured neurons

Significance

Copper is traditionally regarded as a static, tightly bound cofactor in enzymes, but emerging data link more-loosely bound pools to cell signaling. Here we use molecular imaging to identify a role for copper in the brain as a modulator of spontaneous activity of developing neural circuits. First, we directly visualized a labile, loosely bound copper pool in hippocampal neurons and retinal tissue with a newly developed Copper Fluor-3 (CF3) indicator. We then used two-photon calcium imaging as readout of spontaneous activity to show that disruption of labile copper stores by acute chelation or genetic knockdown of the CTR1 (copper transporter 1) copper channel alters the frequency and spatial propagation of neural activity. The results establish the requirement for copper in a fundamental, dynamic property of brain circuitry.

Author contributions: S.C.D., A.F., J.C., C.I.N., M.B.F., and C.J.C. designed research; S.C.D., A.F., J.C., C.I.N., and A.T.A. performed research; J.C., A.T.A., C.S.O., K.M.R.-T., J.P., and C.M.W. contributed new reagents/analytic tools; S.C.D., A.F., and J.C. analyzed data; and S.C.D., A.F., M.B.F., and C.J.C. wrote the paper.

Conflict of interest statement: A patent application has been filed for the fluorescent copper sensors.

This article is a PNAS Direct Submission.

[1]S.C.D., A.F., and J.C. contributed equally to this work.

[2]To whom correspondence should be addressed. Email: chrischang@berkeley.edu.

This article contains supporting information online at www.pnas.org/lookup/suppl/doi:10.1073/pnas.1409796111/-/DCSupplemental.

activated by exogenous chemical depolarization agents mobilize pools of copper from their somatic cell bodies to peripheral processes in a calcium-dependent manner (29). Encouraged by these findings, we sought to probe loosely bound copper pools in higher neuronal tissue models and study their roles in regulating neural circuits under basal conditions with a molecular imaging approach. However, initial attempts to use CS3 and other available copper indicators to reliably visualize labile copper stores in tissue were unsuccessful, despite their utility in a wide range of cell culture models (29–41). We speculated that the relative hydrophobicity of BODIPY dyes could potentially limit their utility in thicker biological specimens due to localization and aggregation effects (30, 42, 43). This situation is unsurprising, as the invention of fluorescent probes is a developing technology and not every probe can be used with the same efficacy in every cell type. In particular, the requirement for careful synthesis, purification, and handling of CS3 due to its relatively short shelf life, even in solid form (41), led us to explore alternative sensor platforms for copper detection. To address this technological gap, we designed and synthesized a family of fluorescent copper sensors, Copper Rhodols 1–5 (CR1–5), based on the rhodol scaffold as shown in Fig. 1*A*. Rhodols are hybrid fluorescein–rhodamine dyes that offer improved hydrophilicity over their BODIPY counterparts yet maintain good optical brightness, photostability, and insensitivity to changes in the physiological pH range (44). These properties allow them to be used for both one- and two-photon microscopy, where the latter technique expands their utility for imaging tissue and other thicker specimens (45).

Beginning with the most responsive sensor of the series, Copper Rhodol-3 (CR3), we strategically made a methyl to trifluoromethyl substitution on the bottom ring receptor to afford CF3, which exhibits enhanced photophysical properties (*vide infra*). Moreover, a set of matched control rhodols, Control Copper Rhodol-3 (Ctrl-CR3) and Ctrl-CF3, that lack a copper-responsive receptor were prepared to distinguish between receptor-dependent and dye-dependent responses. Specifically, the thioether-rich receptor arms for Cu^+ recognition in CR3 and CF3 were replaced by isostructural octyl groups in Ctrl-CR3 and Ctrl-CF3 that mimic the size, shape, and hydrophobicity of thioethers but do not bind copper. The syntheses of the fluorescent copper indicators, CR3 and CF3, as well as the control analogs, Ctrl-CR3 and Ctrl-CF3, are depicted in Fig. 1*B* and Fig. S1*A*. The preparation and characterization of all other copper sensors are described in *SI Materials and Methods*. The general syntheses proceeded through addition of the aryl lithium species, derived from the bromoarene via lithium halogen exchange, to the appropriate xanthone. Briefly, xanthone **3** was accessed in two steps starting from the nucleophilic aromatic substitution of **1** with stoichiometric pyrrolidine to give the monopyrrolidino xanthone **2**. Subsequent one-pot conversion to xanthone **3** involved hydrolysis of the triflate with tetraethylammonium hydroxide, followed by protection of the phenol with *tert*-butyldimethylsilyl chloride. The bromobenzene precursors **8** and **12** were prepared from the quantitative reduction of methyl 4-bromo-3-methylbenzoate **4** and methyl 4-bromo-3-(trifluoromethyl)benzoate **9** with lithium aluminum hydride to afford benzyl alcohols **5** and **10**, respectively. The benzyl chlorides **6** and **11** were accessed, respectively, by refluxing **5** and **10** in solutions of thionyl chloride in dichloromethane. Finally, incorporation of the thioether-rich binding domain via nucleophilic displacement of the benzyl chloride with bis(2-((2-(ethylthio)ethyl)thio)ethyl)amine **7** afforded bromobenzenes **8** and **12**, respectively. Likewise, substitution with dioctylamine allowed for the preparation of the nonresponsive copper control precursors **14** and **15**, respectively. The appropriate xanthone and bromobenzene synthons were then coupled to give the final CR3 and CF3 probes and their control compounds.

We reasoned that replacement of the methyl substituent on the bottom ring receptor of CR3 with a trifluoromethyl group would result in enhancements in dynamic range and optical brightness by (*i*) providing greater steric bulk to minimize nonradiative decay by rotational motions between the receptor-containing aryl and xanthene rings and (*ii*) enhancing quenching of the unbound state by photoinduced electron transfer and/or alleviating quenching related to charge-transfer mechanisms by decreasing electron density on the receptor-containing aryl ring. Indeed, CR3 gives a 13-fold turn-on fluorescence enhancement upon binding to Cu^+, but CF3 responds to Cu^+ with a 40-fold emission increase (Fig. 2 *A* and *C*) with a 20-nM detection limit (Fig. S3*E*). Both sensors exhibit high selectivity for Cu^+, even in the presence of physiologically relevant concentrations of competing metal ions (Fig. 2 *B* and *D*). The fluorescence responses of CR3 and CF3 to Cu^+ are not affected by the presence of 2 mM Ca^{2+}, Mg^{2+}, and Zn^{2+}, nor do these metal ions cause increases in observed fluorescence signals. Moreover, other biologically abundant transition metal ions (50 μM Mn^{2+}, Fe^{2+}, Co^{2+}, Ni^{2+}, or Cu^{2+}) do not trigger false positives nor do they interfere with Cu^+-induced fluorescence enhancements for CR3 and CF3. Notably, Cu^{2+} data show that both indicators maintain oxidation state specificity for Cu^+ over

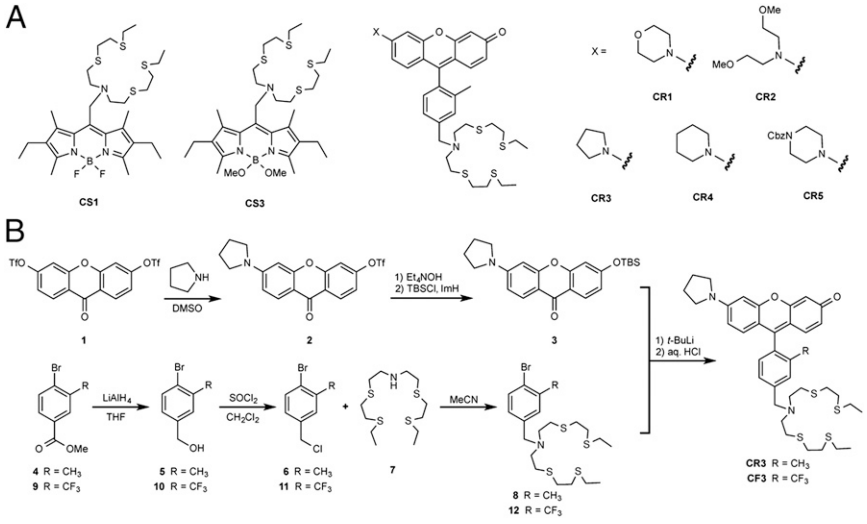

Fig. 1. Preparation and characterization of CR3 and CF3. (*A*) Schematic of BODIPY- and rhodol-based copper sensors. (*B*) Synthetic scheme of CR3 and CF3.

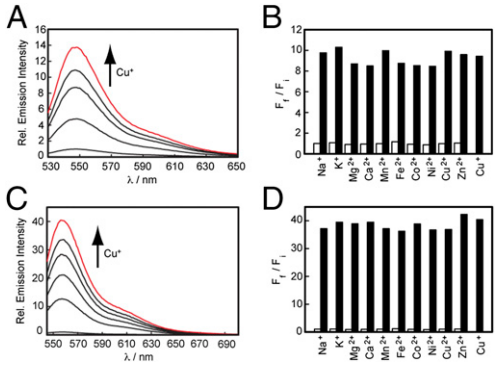

Fig. 2. Plot of fluorescence increase of 2 μM (*A*) CR3 and (*C*) CF3 to Cu^{+}. Points are shown for 0 μM, 0.4 μM, 0.8 μM, 1.2 μM, 1.6 μM, and 2 μM Cu^{+}. Excitation was provided at 534 nm and collected from 545 to 700 nm. Fluorescence responses of (*B*) CR3 and (*D*) CF3 to various metal ions. Bars represent the final integrated fluorescence response (F_f) over the initial integrated emission (F_i). White bars represent the addition of an excess of the indicated metal ion (2 mM for Na^{+}, K^{+}, Mg^{2+}, Ca^{2+}, and Zn^{2+}; 50 μM for all other cations) to a 2 μM solution of CR3 or CF3. Black bars represent subsequent addition of 2 μM Cu^{+} to the solution. Excitation was provided at 534 nm, and collected emission was integrated from 545 nm to 700 nm.

Cu^{2+}. Additionally, the Ctrl-CR3 and Ctrl-CF3 probes do not respond to Cu^{+} or any other metal ions (Table S1). Finally, based on determination of partition coefficients, we find that CR3 and CF3 are more hydrophilic (log D = 0.96 for CR3, 1.15 for CF3) compared with the BODIPY counterpart CS3 (log D = 3.46), potentially enabling the broader use of these CR3/CF3 platforms in both cell and tissue specimens (Table S1). Further in vitro experiments establish that CF3, but not Ctrl-CF3, is able to respond to copper in the presence of artificial lipid vesicles (Fig. S3 *F–I*), BSA as a model protein (Fig. S3*J*), and millimolar levels of glutathione (GSH) (Fig. S3 *K* and *L*), an abundant competing cellular ligand for Cu(I) (apparent $K_d = 9 \times 10^{-12}$ assuming the major species is a 1:1 Cu:GSH complex) (46, 47), as well as cell lysates that contain all of these components (Fig. S3*M*).

Molecular Imaging with CF3 Revealed Pools of Loosely Bound Copper in Cultured Dissociated Hippocampal Neurons and Acutely Isolated Retinal Tissue. The enhanced sensitivity and hydrophilicity of CF3 enabled the study of exchangeable Cu^{+} stores in neuronal circuits formed from dissociated hippocampal cultures and retinal tissue models using confocal or two-photon scanning imaging (Fig. 3 and Fig. S8*A*). Dissociated hippocampal neurons (days in vitro (DIV) 10–13) loaded with CF3 for 20 min followed by perfusion with buffered saline [Hank's Balanced Salt Solution (HBSS)] (see *SI Materials and Methods*) and imaging with two-photon confocal microscopy showed a diffuse intracellular fluorescent signal (Fig. 3*A*). Acute bath application of the cell-impermeable copper chelator bathocuproine disulfonate (BCS) to the same field of neurons showed a patent decrease in intracellular fluorescence intensity. The data suggest that CF3 is capable of detecting basal, endogenous pools of labile copper in neurons and their depletion by on-stage pharmacological treatments within minutes of chelation (Fig. 3*B*), as BCS has a higher affinity for Cu^{+} compared with CF3 (1×10^{-20} vs. 3.3×10^{-13}) and therefore alters intracellular pools of loosely bound copper pools by sequestering extracellular copper stores (48). Notably, the application of Ctrl-CF3, which possesses an identical fluorophore but lacks the copper responsive binding element, under the same experimental conditions showed no change in fluorescence intensity upon treatment with BCS. This critical control experiment confirmed that the observed BCS-induced decreases in CF3 fluorescence were not due to photobleaching and/or dye leakage effects. Moreover, BCS was not observed to induce general oxidative stress in hippocampal cultures (Fig. S8*C*), further supporting that observed changes in CF3 intensity are copper dependent. Because GSH is an abundant species in cells and a potential competing ligand for labile copper, we speculate that CF3 could exchange or form a ternary complex with GSH-bound copper (46, 47). Indeed, intracellular CF3 fluorescence in hippocampal neurons decreased upon treatment with the cell-permeable copper chelator GSH monoethyl ester (GSH-MEE) (Fig. S8*B*), suggesting that CF3 can reversibly respond to changes in the GSH-dependent copper pool.

Next, acutely isolated retinal tissues (P10–P13) were loaded with CF3 and the fluorescence intensity was imaged from the ganglion cell layer (GCL) using a scanning two-photon microscope (Fig. S9*A* and Fig. 3*C*). The retina consists of distinct cellular layers that contain neuronal somata and are separated by two plexiform layers that contain the processes and synapses between these neurons. CF3 labeled the intracellular space of the innermost cell layer, the GCL, and responded to a decrease in the pool of loosely bound Cu^{+} upon perfusion with BCS (Fig. 3*C*). Similarly, loading retinas with Ctrl-CF3 followed by extracellular copper chelation did not result in a change in fluorescence, indicating that two-photon imaging of CF3 can be used to report on an endogenous pool of loosely bound Cu^{+} (Fig. 3*D*).

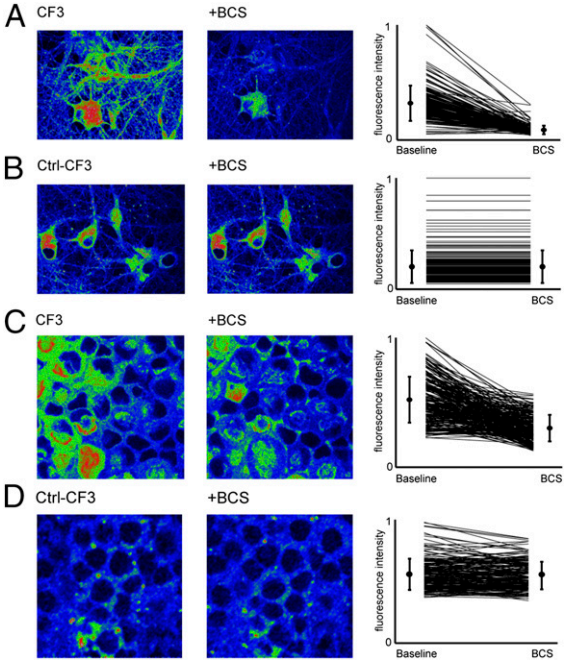

Fig. 3. Live two-photon imaging of CF3 in cultured dissociated hippocampal neurons and retinal tissue shows that acute BCS treatment alters intracellular labile Cu^{+}. Representative images are shown of hippocampal neurons were stained with (*A*) 2 μM CF3 (CF3: baseline normalized mean = 0.32, SD = 0.15; after BCS: mean = 0.088, SD = 0.038; n = 192 15-μm squares) or (*B*) Ctrl-CF3 for 20 min with subsequent recording of baseline fluorescence followed by 30 min BCS perfusion (Ctrl-CF3: baseline normalized mean = 0.20, SD = 0.15; after BCS: mean = 0.20, SD = 0.15; n = 192 15-μm squares). Net changes in fluorescence brightness are quantified on the right with paired lines representing nonoverlapping 15-μM square regions of the field of view. Representative images of retinal neurons bolus loaded with (*C*) CF3 (CF3: baseline normalized mean = 0.49, SD = 0.16; after BCS: mean = 0.26, SD = 0.10; n = 256 15-μm squares) or (*D*) Ctrl-CF3 followed by 30 min BCS perfusion (Ctrl-CF3: baseline normalized mean = 0.57, SD = 0.13; after BCS: mean = 0.56, SD = 0.11; n = 256 15-μm squares). Net changes in fluorescence brightness are quantified on the right, with paired lines representing nonoverlapping 15-μm square regions of the field of view.

Taken together, the data suggest that CF3 enables identification of loosely bound copper pools at endogenous levels in both dissociated neuronal cultures and in brain tissue, and that the membrane-impermeable copper chelator BCS alters the extracellular pool of loosely bound Cu^{+}, which subsequently depletes the intracellular pool. As such, we reasoned that dynamic disruptions in loosely bound Cu^{+} stores may also result in alterations to spontaneous activity in neural networks.

Modulation of Spontaneous Activity with Acute Extracellular Copper Chelation in Dissociated Hippocampal Neurons. First, we examined the effects of BCS treatment on spontaneous activity of a network of cultured hippocampal neurons using both confocal and two-photon based calcium imaging. Cultures of embryonic neurons (DIV 12–15) were incubated with the Ca^{2+} indicator, Oregon Green BAPTA-1 AM (OGB). These dissociated hippocampal cultures, which consist of neurons and glia, exhibited temporally uncorrelated calcium transients (Fig. 4*A*). Bath application of the copper chelator BCS in a dose-dependent manner (5–200 μM) triggered increases in the correlations between calcium transients (Fig. S8*D* and Fig. 4*B*). Importantly, uncorrelated calcium transients were restored upon washout of BCS, showing that this modulation is reversible (Fig. S8*E*). To compare quantitatively the correlated events, we computed cross-correlations based upon the percentage of imaged cells that exhibited spontaneous calcium transients surrounding the peak event (see *SI Materials and Methods*). In control conditions, a lower percentage of cells exhibited correlated calcium transients (Fig. 4*B*). These data are consistent with the model that disrupting loosely bound copper stores by acute chelation increases the excitability of the network, leading to a reversible increase in correlated activity (49).

Pharmacological Manipulation of Endogenous Pools of Loosely Bound Copper Alters Spontaneous Activity in the Developing Retina. Next, we studied spontaneous activity in the developing retina, a well-understood model for correlated spontaneous activity during development (50, 51). Before the maturation of the light responses, the retina exhibits spontaneous correlated activity, termed retinal waves. To investigate the effects of copper chelation on retinal waves, we used two-photon calcium imaging to record from the neurons in the GCL in which resides a pool of exchangeable copper that was altered by acute BCS treatment (Fig. 5). Retinas were acutely isolated from P10–P13 mice and bolus loaded with OGB as previously described (52). Spontaneous calcium transients propagated across the GCL with a well-defined periodic frequency (Fig. 5 *A* and *B*). Acute bath application

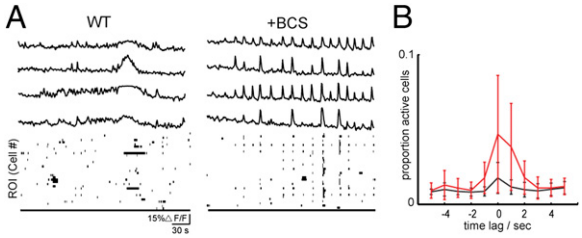

Fig. 4. Copper chelation with BCS increases the correlated calcium transients in dissociated hippocampal culture. (*A*) Sample ΔF/F traces from averaged regions from four different cells stained with OGB. Each trace row corresponds to the same in cell in control solution first (*Left*) followed by chelation with 200 μM BCS (*Right*). Binary plots (*Bottom*) show entire network activity, where a black point corresponds to a cell with a calcium transient above threshold. (*B*) Mean and SD across cells of cross-correlation during times of high-synchronized firing ($n = 3$ cultures). When a time point was identified as having more than 10% of cells above threshold, the proportion of cells that were above threshold was calculated for 5 s before and after. A flat line indicates uniform, random transients. WT (black) and acute 200 μM BCS wash-in (red).

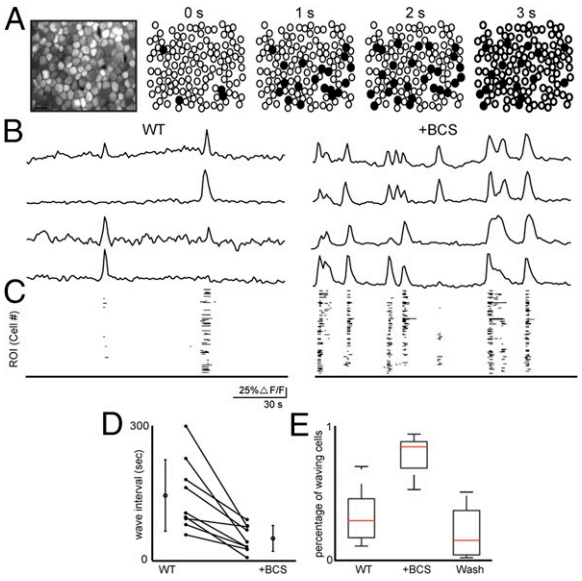

Fig. 5. Copper chelation increases wave frequency and cell participation levels of correlated spontaneous activity in the developing retina. (*A*) Example of retinal wave propagation in the GCL observed with two-photon calcium imaging at a frame rat of 1 Hz. Leftmost image is the retinal sample loaded with OGB. Circles are identified cells where black indicates cells with above-threshold ΔF/F in that frame. (*B*) Sample ΔF/F traces from averaged regions within four different cells. Each trace row corresponds to the same cell in control solution first (*Left*) followed by chelation with 200 μM BCS (*Right*). (*C*) Binary plots of neuronal calcium transients exceeding threshold for all cells in the field of view. (*D*) Summary of effects of BCS on interevent interval where lines connect values of average wave interval for one retina in control versus chelation with BCS. Open circles are group means, and bars are SD. (*E*) Summary of effects of BCS on proportion of cells that are active during waves ($n = 9$ retinas, $P < 0.001$, Kruskal–Wallis test). Box boundaries indicate upper and lower quartiles, with the median plotted in red with whiskers extending to the most extreme values that are still considered not to be outliers.

of 200 μM BCS increased the frequency of waves; the median interevent interval decreased for BCS-treated retinas (median, upper/lower quartile; control: 100 s, 60/130, $n = 17$ intervals; BCS: 29 s, 17/58 s, $n = 51$ intervals; wash wave interval: 60 s, 17/58, $n = 6$ intervals) (Fig. 5 *C* and *D*). In addition, BCS increased the percentage of GCL neurons that depolarized during correlated activity and this effect was reversible upon BCS washout (median, upper/lower quartile; control: 26%, 8.9/34; BCS: 75%, 56/78; wash: 12%, 1/20, $n = 9$ retinas; Kruskal–Wallis test, $P < 0.001$) (Fig. 5*E*). To confirm that BCS is functioning by altering labile copper concentrations, we applied ATN-224, a membrane-permeable copper chelator that is chemically distinct from BCS and irreversibly alters both intracellular and extracellular copper stores. Consistent with the BCS results, bath application of ATN-224 (15 μM) increased wave frequency in the mouse retina (median, upper/lower quartile; control: 153 s, 82/168, $n = 7$ intervals; ATN-224: 34 s, 16/74, $n = 13$ intervals; Wilcoxon signed-rank test, $P < 0.05$; Fig. S9*D*). BCS was the primary copper chelator used because of its cell-impermeable nature, which allows for reversible application to tissue and offers a better mimic of a genetic knockout of the membrane-bound CTR1 protein that controls copper entry into cells from the extracellular face. Similar to what we observed in the hippocampal cultures, the disruption of endogenous pools of loosely bound copper by acute addition of chelators increases excitability of retinal circuits, suggesting a role for copper in regulating spontaneous activity.

Spontaneous Activity Is Altered in CTR1$^{+/-}$ Retinal Tissue. To probe the effects of genetic, long-term disruption of total copper in the developing retina, as well as provide a molecular target for dynamic regulation of copper cycling, we compared our findings from WT mice to retinas isolated from transgenic mice that have heterozygote expression of the CTR1 copper ion channel (CTR1$^{+/-}$), which has ∼50% less copper in the nervous system compared with WT CTR1$^{+/+}$ mice; we note that the homozygous CTR1$^{-/-}$ mice are embryonic lethal and cannot be used for such studies (53). First, we tested the total copper content in eyes isolated from WT and CTR1$^{+/-}$ by inductively coupled plasma mass spectrometry (ICP-MS). Eyes isolated from CTR1$^{+/-}$ mice accumulated less copper compared with WT (Cu/S with SD; CTR1$^{+/+}$ Cu/S = 0.00030 ± 0.00003; CTR1$^{+/-}$ Cu/S = 0.00025 ± 0.00002; $n \geq 6$ eyes). We also confirmed that there was a patent reduction in CTR1 expression in CTR1$^{+/-}$ mice retinas by Western blot (Fig. 6*F*). The direct ICP-MS measurements are supported by secondary imaging experiments, where CTR1$^{+/-}$ retinas loaded with CF3 show lower levels of fluorescence compared with WT retinas stained with this dye under identical conditions, whereas WT and CTR1$^{+/-}$ retinas loaded with the Ctrl-CF3 dye that does not respond to copper show comparable fluorescence signals (Fig. S9*C*). Retinas from P11 CTR1$^{+/-}$ mice exhibited spontaneous calcium transients as observed in WT mice (Fig. 6 *A* and *B*). However, similar to what was observed for BCS-treated WT retinas, waves in CTR1$^{+/-}$ retinas were more frequent than littermate controls (median interevent interval upper/lower quartile; CTR1$^{+/+}$: 95 s, 76/149, n = 33 intervals; CTR1$^{+/-}$: 22 s, 14/32, n = 129 intervals; Wilcoxon signed-rank test, $P < 0.001$) and the percentage of depolarized cells increased (median, upper/lower quartile; control WT: 27%, 16/51, n = 18 retinas; CTR1$^{+/-}$: 67%, 17/68, n = 16 retinas; Wilcoxon signed-rank test, $P < 0.001$) (Fig. 6 *D* and *E*). Taken together, the data establish that disruptions of endogenous copper pools by genetic knockdown of the copper ion channel CTR1 or acute treatment with chelators like BCS or ATN-224 increase network excitability in both hippocampal culture and intact retinas. The observed changes to spontaneous neuronal activity in both systems suggest a general, fundamental role for copper in modulating spontaneous activity in developing neural circuits and identify CTR1 as a molecular target for mediating this effect through maintenance of extracellular and intracellular pools of loosely bound copper.

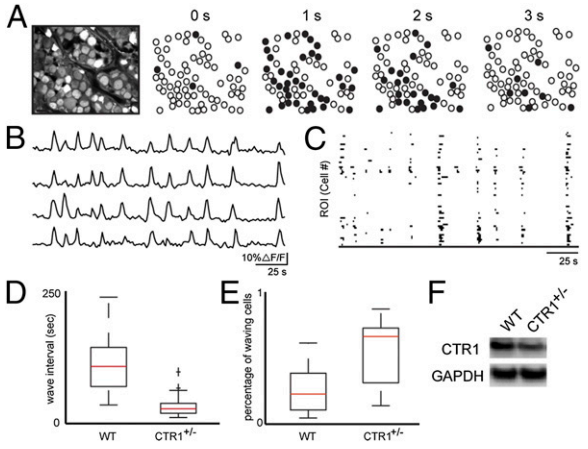

Fig. 6. Partial knockdown of CTR1 in the retina increases wave frequency and cell participation in retinal waves. (*A*) Example of wave propagation in the GCL observed with two-photon calcium imaging at a frame rate of 1 Hz. Leftmost image is the retinal sample loaded with OGB. Circles are identified cells where black indicates cells with ΔF/F greater than 15% in that frame. (*B*) Sample ΔF/F traces from averaged regions within four different cells. Each trace row represents a different cell. (*C*) Binary plots of neuronal calcium transients greater than 15% ΔF/F for all cells in the field of view. (*D*) Summary of differences between WT and CTR1$^{+/-}$ retina on interevent interval (WT: n = 33 waves; CTR1$^{+/-}$: n = 129 waves). (*E*) Summary of differences between WT and CTR1$^{+/-}$ retina on proportion of cells that are active during waves (WT: n = 18 retinas; CTR1$^{+/-}$: n = 16 retinas). Box boundaries indicate upper and lower quartiles, with the median plotted in red with whiskers extending to the most extreme values that are still considered not to be outliers. (*F*) Representative Western blot of CTR1 expression in WT and CTR1$^{+/-}$ developing retina. GAPDH was used as a loading control.

Concluding Remarks

The utilization of metals for dynamic signaling purposes in the brain and other biological systems has largely focused on mobile fluxes of redox-inactive alkali and alkaline earth metals such as sodium, potassium, and calcium, whereas redox-active metals have been viewed primarily as static metabolic cofactors. In this work, we have shown that copper is an endogenous and dynamic mediator of spontaneous activity in neural circuits. We showed that CF3, a fluorescent copper sensor with improved hydrophilicity, high selectivity and sensitivity to labile Cu^+, and ability to be visualized using both confocal and two-photon imaging methods, when used along with the matched control dye Ctrl-CF3 that lacks sensitivity to copper, enabled the identification of loosely bound copper pools that are exchanged across the cell membrane in dissociated neuronal cultures. We further demonstrated that neural activity can be modulated by acute addition of the membrane-impermeable copper chelator BCS. Specifically, we have shown that acute copper chelation in a dose-dependent manner in dissociated hippocampal culture and intact developing retina increased the cell participation and frequency of calcium transients during spontaneous activity. Moreover, modulation of cellular copper levels through genetic knockdown of the copper ion channel CTR1 led to a similar increase in synchronization of calcium transients, indicating that this protein is involved in dynamic regulation of copper signaling, which in turn affects neural activity.

Our results suggest that endogenous intracellular and extracellular pools of loosely bound copper are used to regulate levels of spontaneous activity during neural circuit development through CTR1, which could potentially include regulation of intracellular and extracellular copper concentrations, cell surface copper recycling, and/or loading of copper onto extracellular membrane receptors involved in calcium uptake. Indeed, previous experiments suggest that copper influences synaptic transmission by modulation of a variety of targets, including NMDA receptors (12–14), $GABA_A$ receptors (54), and voltage-gated calcium channels (55). To begin exploring mechanisms for the observed increase in spontaneous activity with alterations in copper buffering, we bath applied the NMDA receptor antagonist (2*R*)-amino-5-phosphonovaleric acid APV (50 μM) to both WT retinas treated with BCS and retinas isolated from CTR1$^{+/-}$ mice (Fig. S9 *E*–*H*). In both cases, the presence of APV abolished the effects of BCS, restoring activity to control levels. The data suggest a connection between copper and NMDA receptor activity (12, 13).

Correlated spontaneous activity is critical for the normal development of synapses and circuits (50, 56, 57), and therefore regulation of this activity by copper has implications for developmental diseases such as Menkes disease. In addition, our data implicate Cu^+ signaling in neuronal signaling, suggesting that alterations in brain copper homeostasis in genetic disorders like Wilson's disease, as well as more complex neurodegenerative diseases such as Alzheimer's and Huntington's diseases and prion encephalopathies that are linked to copper mismanagement, can contribute to misregulation of cell–cell communication. Finally, these findings highlight the continuing need to develop molecular imaging probes as pilot screening tools to help uncover unique and unexplored metal biology in living systems and support a broader view for transition metals in cell signaling.

Materials and Methods

Materials and procedures are described in *SI Materials and Methods*. Included are synthesis and characterization of compounds. In vitro spectroscopic evaluation of sensors and biochemical experiments are also presented. Imaging in cell and tissue models, along with pharmacological and genetic manipulations, are documented. All procedures were approved by the Institutional Animal Care and Use Committee of the University of California, Berkeley, CA and conformed with guidelines of the National Institutes of Health *Guide for the Care and Use of Laboratory Animals,* the Public Health Service Policy, and the Society for Neuroscience Policy on the Use of Animals in Neuroscience Research.

ACKNOWLEDGMENTS. We thank Prof. T. Hirayama and Mr. S. Farhi for helpful discussions regarding synthesis, Dr. D. Domaille for help in setting up initial calcium imaging experiments, Ms. C. Ackerman for help with ICP-MS sample preparation, Prof. D. Thiele for a breeding pair of CTR1$^{+/-}$ mice, Dr. A. Mazar for generously providing ATN-224, and Prof. E. Isacoff and his laboratory for providing technical expertise and helpful discussions. We thank the National Institutes of Health (NIH) for funding this work [R01 GM 79465 (to C.J.C.) and R01 EY013528 (to M.B.F.)]. C.J.C. is an Investigator with the Howard Hughes Medical Institute. J.C. acknowledges the Human Frontier Sciences Program for a postdoctoral fellowship. A.T.A., C.S.O., and K.M.R.-T. were partially supported by Chemical Biology Training Grant T32 GM066698 from NIH. A.T.A. thanks the National Science Foundation for a graduate fellowship.

1. Bush AI (2000) Metals and neuroscience. *Curr Opin Chem Biol* 4(2):184–191.
2. Burdette SC, Lippard SJ (2003) Meeting of the minds: Metalloneurochemistry. *Proc Natl Acad Sci USA* 100(7):3605–3610.
3. Que EL, Domaille DW, Chang CJ (2008) Metals in neurobiology: Probing their chemistry and biology with molecular imaging. *Chem Rev* 108(5):1517–1549.
4. Dickinson BC, Chang CJ (2011) Chemistry and biology of reactive oxygen species in signaling or stress responses. *Nat Chem Biol* 7(8):504–511.
5. Barnham KJ, Masters CL, Bush AI (2004) Neurodegenerative diseases and oxidative stress. *Nat Rev Drug Discov* 3(3):205–214.
6. Savelieff MG, Lee S, Liu Y, Lim MH (2013) Untangling amyloid-β, tau, and metals in Alzheimer's disease. *ACS Chem Biol* 8(5):856–865.
7. Lutsenko S, Bhattacharjee A, Hubbard AL (2010) Copper handling machinery of the brain. *Metallomics* 2(9):596–608.
8. Gaier ED, Eipper BA, Mains RE (2013) Copper signaling in the mammalian nervous system: Synaptic effects. *J Neurosci Res* 91(1):2–19.
9. Kim BE, Nevitt T, Thiele DJ (2008) Mechanisms for copper acquisition, distribution and regulation. *Nat Chem Biol* 4(3):176–185.
10. Robinson NJ, Winge DR (2010) Copper metallochaperones. *Annu Rev Biochem* 79: 537–562.
11. Huffman DL, O'Halloran TV (2001) Function, structure, and mechanism of intracellular copper trafficking proteins. *Annu Rev Biochem* 70:677–701.
12. Schlief ML, Craig AM, Gitlin JD (2005) NMDA receptor activation mediates copper homeostasis in hippocampal neurons. *J Neurosci* 25(1):239–246.
13. Schlief ML, West T, Craig AM, Holtzman DM, Gitlin JD (2006) Role of the Menkes copper-transporting ATPase in NMDA receptor-mediated neuronal toxicity. *Proc Natl Acad Sci USA* 103(40):14919–14924.
14. You H, et al. (2012) Aβ neurotoxicity depends on interactions between copper ions, prion protein, and N-methyl-D-aspartate receptors. *Proc Natl Acad Sci USA* 109(5): 1737–1742.
15. Kaler SG (2011) ATP7A-related copper transport diseases-emerging concepts and future trends. *Nat Rev Neurol* 7(1):15–29.
16. Camakaris J, Voskoboinik I, Mercer JF (1999) Molecular mechanisms of copper homeostasis. *Biochem Biophys Res Commun* 261(2):225–232.
17. Lutsenko S, Barnes NL, Bartee MY, Dmitriev OY (2007) Function and regulation of human copper-transporting ATPases. *Physiol Rev* 87(3):1011–1046.
18. Beckman JS, Estévez AG, Crow JP, Barbeito L (2001) Superoxide dismutase and the death of motoneurons in ALS. *Trends Neurosci* 24(11 Suppl):S15–S20.
19. Valentine JS, Hart PJ (2003) Misfolded CuZnSOD and amyotrophic lateral sclerosis. *Proc Natl Acad Sci USA* 100(7):3617–3622.
20. Adlard PA, et al. (2008) Rapid restoration of cognition in Alzheimer's transgenic mice with 8-hydroxy quinoline analogs is associated with decreased interstitial Abeta. *Neuron* 59(1):43–55.
21. Sparks DL, Schreurs BG (2003) Trace amounts of copper in water induce beta-amyloid plaques and learning deficits in a rabbit model of Alzheimer's disease. *Proc Natl Acad Sci USA* 100(19):11065–11069.
22. Singh I, et al. (2013) Low levels of copper disrupt brain amyloid-β homeostasis by altering its production and clearance. *Proc Natl Acad Sci USA* 110(36):14771–14776.
23. Fox JH, et al. (2007) Mechanisms of copper ion mediated Huntington's disease progression. *PLoS ONE* 2(3):e334.
24. Xiao G, Fan Q, Wang X, Zhou B (2013) Huntington disease arises from a combinatory toxicity of polyglutamine and copper binding. *Proc Natl Acad Sci USA* 110(37): 14995–15000.
25. Brown DR, et al. (1997) The cellular prion protein binds copper in vivo. *Nature* 390(6661): 684–687.
26. Siggs OM, et al. (2012) Disruption of copper homeostasis due to a mutation of Atp7a delays the onset of prion disease. *Proc Natl Acad Sci USA* 109(34):13733–13738.
27. Hartter DE, Barnea A (1988) Evidence for release of copper in the brain: Depolarization-induced release of newly taken-up 67copper. *Synapse* 2(4):412–415.
28. Duan X, et al. (2012) Crucial role of copper in detection of metal-coordinating odorants. *Proc Natl Acad Sci USA* 109(9):3492–3497.
29. Dodani SC, et al. (2011) Calcium-dependent copper redistributions in neuronal cells revealed by a fluorescent copper sensor and X-ray fluorescence microscopy. *Proc Natl Acad Sci USA* 108(15):5980–5985.
30. Zeng L, Miller EW, Pralle A, Isacoff EY, Chang CJ (2006) A selective turn-on fluorescent sensor for imaging copper in living cells. *J Am Chem Soc* 128(1):10–11.
31. Dodani SC, Leary SC, Cobine PA, Winge DR, Chang CJ (2011) A targetable fluorescent sensor reveals that copper-deficient SCO1 and SCO2 patient cells prioritize mitochondrial copper homeostasis. *J Am Chem Soc* 133(22):8606–8616.
32. Quaranta D, et al. (2011) Mechanisms of contact-mediated killing of yeast cells on dry metallic copper surfaces. *Appl Environ Microbiol* 77(2):416–426.
33. Espírito Santo C, et al. (2011) Bacterial killing by dry metallic copper surfaces. *Appl Environ Microbiol* 77(3):794–802.
34. Beaudoin J, et al. (2011) Mfc1 is a novel forespore membrane copper transporter in meiotic and sporulating cells. *J Biol Chem* 286(39):34356–34372.
35. Bernal M, et al. (2012) Transcriptome sequencing identifies SPL7-regulated copper acquisition genes FRO4/FRO5 and the copper dependence of iron homeostasis in Arabidopsis. *Plant Cell* 24(2):738–761.
36. Cusick KD, et al. (2012) Inhibition of copper uptake in yeast reveals the copper transporter Ctr1p as a potential molecular target of saxitoxin. *Environ Sci Technol* 46(5):2959–2966.
37. Hao Z, et al. (2014) The multiple antibiotic resistance regulator MarR is a copper sensor in *Escherichia coli*. *Nat Chem Biol* 10(1):21–28.
38. Huang CP, Fofana M, Chan J, Chang CJ, Howell SB (2014) Copper transporter 2 regulates intracellular copper and sensitivity to cisplatin. *Metallomics* 6(3):654–661.
39. Polishchuk EV, et al. (2014) Wilson disease protein ATP7B utilizes lysosomal exocytosis to maintain copper homeostasis. *Dev Cell* 29(6):686–700.
40. Kashyap DR, et al. (2014) Peptidoglycan recognition proteins kill bacteria by inducing oxidative, thiol, and metal stress. *PLoS Pathog* 10(7):e1004280.
41. Hong-Hermesdorf A, et al. (2014) Selective sub-cellular visualization of trace metals identifies dynamic sites of Cu accumulation in *Chlamydomonas*. *Nat Chem Biol*, in press.
42. Romieu A, et al. (2013) The first comparative study of the ability of different hydrophilic groups to water-solubilise fluorescent BODIPY dyes. *New J Chem* 37(4):1016–1027.
43. Morgan MT, Bagchi P, Fahrni CJ (2011) Designed to dissolve: Suppression of colloidal aggregation of Cu(I)-selective fluorescent probes in aqueous buffer and in-gel detection of a metallochaperone. *J Am Chem Soc* 133(40):15906–15909.
44. Whitaker JE, et al. (1992) Fluorescent rhodol derivatives: Versatile, photostable labels and tracers. *Anal Biochem* 207(2):267–279.
45. Lim CS, et al. (2011) A copper(I)-ion selective two-photon fluorescent probe for in vivo imaging. *Chem Commun (Camb)* 47(25):7146–7148.
46. Corazza A, Harvey I, Sadler PJ (1996) 1H,13C-NMR and X-ray absorption studies of copper(I) glutathione complexes. *Eur J Biochem* 236(2):697–705.
47. Banci L, et al. (2010) Affinity gradients drive copper to cellular destinations. *Nature* 465(7298):645–648.
48. Cherny RA, et al. (2000) Chelation and intercalation: Complementary properties in a compound for the treatment of Alzheimer's disease. *J Struct Biol* 130(2-3):209–216.
49. Hennig MH, Adams C, Willshaw D, Sernagor E (2009) Early-stage waves in the retinal network emerge close to a critical state transition between local and global functional connectivity. *J Neurosci* 29(4):1077–1086.
50. Huberman AD, Feller MB, Chapman B (2008) Mechanisms underlying development of visual maps and receptive fields. *Annu Rev Neurosci* 31:479–509.
51. Blankenship AG, Feller MB (2010) Mechanisms underlying spontaneous patterned activity in developing neural circuits. *Nat Rev Neurosci* 11(1):18–29.
52. Firl A, Sack GS, Newman ZL, Tani H, Feller MB (2013) Extrasynaptic glutamate and inhibitory neurotransmission modulate ganglion cell participation during glutamatergic retinal waves. *J Neurophysiol* 109(7):1969–1978.
53. Lee J, Prohaska JR, Thiele DJ (2001) Essential role for mammalian copper transporter Ctr1 in copper homeostasis and embryonic development. *Proc Natl Acad Sci USA* 98(12):6842–6847.
54. Peters C, et al. (2011) Biphasic effects of copper on neurotransmission in rat hippocampal neurons. *J Neurochem* 119(1):78–88.
55. Shcheglovitov A, et al. (2012) Molecular and biophysical basis of glutamate and trace metal modulation of voltage-gated Ca(v)2.3 calcium channels. *J Gen Physiol* 139(3): 219–234.
56. Moody WJ, Bosma MM (2005) Ion channel development, spontaneous activity, and activity-dependent development in nerve and muscle cells. *Physiol Rev* 85(3):883–941.
57. Mohajerani MH, Cherubini E (2006) Role of giant depolarizing potentials in shaping synaptic current in the developing hippocampus. *Crit Rev Neurobiol* 18(1-2):13–23.